



Linear polarization grating combining a circular polarization grating with a special cycloidal diffractive quarter waveplate

W. CHEN,^{1,2} Z. ZHAO,^{1,2} C. WANG,^{1,2}  H. LI,^{1,2} R. WEI,^{1,2} S. ZHANG,^{1,2} Z. PENG,¹ Y. LIU,¹ Q. WANG,^{1,3} Q. MU,^{1,2,4} AND L. XUAN^{1,2}

¹State Key Laboratory of Applied Optics, Changchun Institute of Optics, Fine Mechanics and Physics, Chinese Academy of Sciences, Changchun 130033, China

²Center of Material Science and Optoelectronics Engineering, University of Chinese Academy of Sciences, Beijing 100049, China

³qdwang@ciomp.ac.cn

⁴muquanquan@ciomp.ac.cn

Abstract: We introduce and demonstrate a switchable novel linear polarization grating (LPG) consisting of a circular polarization grating (CPG) and a special cycloidal diffractive quarter waveplate (CQWP). The CQWP is developed that marvelously matches the polarization-state of beams passing through the CPG. Such an LPG is so polarization-sensitive that it can split an incident linear polarized beam into two proportionally controllable left- or right-handed circularly polarized lights. We establish rigorous simulation model based on finite element method to investigate near-field polarization-state distribution of CPGs. Furthermore, LPGs are demonstrated and the diffraction properties are obtained with simulation and Jones Matrix analysis. The combination of CPGs and CQWPs is achieved with polymerizable liquid crystal. The experimental results of deflection angle and polarization selectivity of LPGs are consistent with those of simulation.

© 2019 Optical Society of America under the terms of the [OSA Open Access Publishing Agreement](#)

1. Introduction

Conventionally, phase or amplitude gratings operate an electromagnetic wave via changing the spatial-varying optical path lengths or transmittance. Pancharatnam studied the concept of a geometrical phase connected to the evolution of the light polarization state [1]. Due to the properties of optical anisotropy and electrical tunability, liquid crystal (LC) has been widely applied in display field [2]. Subsequently the Pancharatnam-Berry [3] (PB) phase devices are proposed by Crawford *et al.*, who have shown a practical way to produce them using technology that is LC-based [4]. The well-known PB phase devices can achieve 100% diffraction under the half-wave delay condition, in other words, zero-order transmission will be zero. So far, several methods are reported to obtain PB phase devices including polarization holography alignments [4–6], electron beam lithography for space-variant subwavelength-carrier surface-relief elements [7], direct-write laser scanning [8], scanning wave photopolymerization [9,10], and the Digital Micro-mirror Device (DMD) based microlithography to control the LC alignments [11]. Recently, a series of LC PB phase devices generating the desired phase profile by spatially varying the LC directors [12–19] have been developed because of their unique optical properties. One of the most interesting PB phase devices is the LC polarization grating (LCPG) [14–16,20,21] which has been studied for many applications, such as wide-angle and nonmechanical beam steering applications [22], polarization converters [23], tunable filters [24], virtual/augmented reality displays [25,26] and micro-displays [27].

In principle, there are two types of LCPGs: active and passive. The active LCPG is made of LC material and can be electronically controlled by the applied voltage [28]. The passive LCPG, also known as the polymer LCPG, consists of a thin LC polymeric film [29,30] whose thickness satisfies what a half-waveplate demands, and theoretically it can obtain 100% diffraction efficiency between +1st and -1st orders [22,31]. In this paper, it mainly refers to the polymer LCPG below. Sometimes LCPGs are called circular polarization gratings (CPG) due to the property that they can split the incident orthogonal circular polarization components as +1st and/or -1st diffraction order lights whose polarization state are flipped into opposite handedness. As far as we know, although LCPGs possess so abundantly extraordinary properties and some polarization splitters [32,33] based PB phase have been proposed, few implementations were reported about polarization splitter based on LCPGs. Inspired by LCPGs, we propose a novel polarization grating, which can deflect special-polarized-directional linearly polarized lights in a single order and can also split circularly polarized lights as +1st and -1st orders. On the other hand, little attention is paid on the concept of quarter waveplate for inhomogeneous polarization beams whose prototype is the polarization grating or one of other PB phase devices with quarter-wave retardation.

In this paper, we demonstrate a compact, light and high-efficient linear polarization grating (LPG). Such an LPG consists of a half-wave retardation LCPG and a special cycloidal diffractive quarter waveplate (CQWP). Unlike CPGs, LPGs can spatially separate orthogonal linear polarization components of incident beams with opposite circular polarization states. It means that there is no need to add extra optical element for polarization state conversion. In section 2, we build a rigorous simulation model to research the polarization-state evolution of LCPGs. Then, we propose a CQWP for vector beams, which can change the polarization-state of near-field output from LCPGs. Next the structure of the LPG is demonstrated and the properties of the LPG are confirmed by Jones Matrix Method and our simulation model respectively. In section 3, we use polarization holography alignments [4,34] to fabricate a few LCPGs and CQWPs. The LPG can be obtained by sticking an LCPG and a CQWP together correctly. In section 4, we discuss the probable difficulty of combining the LCPG and the CQWP to form an LPG. Besides, we experimentally measure the result about polarization selectivity of LPGs.

2. Operation principle and simulation

2.1. Properties and polarization-state evolution of LCPGs

The LC director distribution in an LCPG possesses a spiral pattern of linear anisotropy. Specifically, the structure can be described as an in-plane linear birefringence with an optical symmetry axis that varies with position as

$$\mathbf{n}(x) = \{\sin(\pi x / \Lambda), \cos(\pi x / \Lambda), 0\} \quad (1)$$

where Λ is the half-pitch as shown in Fig. 1(a). The LC director does not change along the y direction. The transfer matrix for an LCPG can be expressed as

$$\mathbf{T} = \mathbf{R}(-\varphi) \cdot \begin{pmatrix} \exp(-i\Gamma/2) & 0 \\ 0 & \exp(i\Gamma/2) \end{pmatrix} \cdot \mathbf{R}(\varphi). \quad (2)$$

where phase retardation $\Gamma = 2\pi\Delta n d / \lambda$, Δn is birefringence, d is the thickness of the LCPG, λ is wavelength in vacuum, \mathbf{R} is the rotation matrix, and $\varphi = \varphi(x) = \pi x / \Lambda$.

We can rewrite Eq. (2) as follows

$$\mathbf{T} = \cos(\Gamma/2) \begin{bmatrix} 1 & 0 \\ 0 & 1 \end{bmatrix} + \frac{1}{2} \sin(\Gamma/2) \left(\exp(i2\varphi) \begin{bmatrix} -i & -1 \\ -1 & i \end{bmatrix} + \exp(-i2\varphi) \begin{bmatrix} -i & 1 \\ 1 & i \end{bmatrix} \right) \quad (3)$$

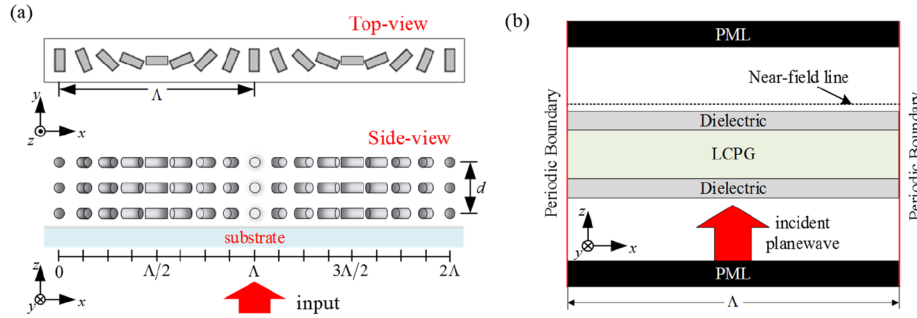


Fig. 1. Concept and simulation of an LCPG. (a) A schematic diagram of the LCPG in side-view and top-view. (b) A layout of FEM simulation space. The simulation space includes only one period of the LCPG.

If the phase retardation satisfies the half-wave condition ($\Delta nd = \lambda/2$), two first orders will be obtained in the output light. Assuming a circularly polarized normal incidence $\begin{pmatrix} E_x \\ E_y \end{pmatrix} = \begin{pmatrix} 1 \\ \pm i \end{pmatrix}$, the output is $\begin{pmatrix} E_x \\ E_y \end{pmatrix} = \begin{pmatrix} 1 \\ \mp i \end{pmatrix}$, and the diffraction angle θ_m of the m th order propagating wave is determined by the grating equation

$$\sin \theta_m = m\lambda / \Lambda. \quad (4)$$

Note that the grating equation is based on a small angle approximation. However, it has been generally accepted because it is like the equation of diffraction gratings.

To investigate the evolution of polarization state and the inner operating mechanism of LCPGs and LPGs, firstly we build a rigorous 2D simulation model using finite element method (FEM). Figure 1(b) illustrates a 2D simulation space for LCPGs analysis, like the layout of the FDTD method proposed by Oh and Escuti [34]. The finite simulation space is implemented by applying the periodic boundary conditions along the x -axis and placing perfectly matched layers (PML) to absorb output beams at the boundaries along z -axis. In order to appropriately isolate the effect of the LCPGs themselves from Fresnel reflection effects, we set a dielectric with the same average refractive index as LC on both sides of the LCPGs. The near-field line is used to monitor the polarization state evolution and calculate far-field diffraction efficiency by vector Fourier transform.

The well-known Poincaré Sphere is a unit sphere, on which any arbitrary polarization state of a plane wave can be graphically represented as a point. Using the Poincaré Sphere, it is convenient to describe how optical elements act upon the polarization of the light wave passing through them. Now, considering an LCPG with half-wave retardation, we monitor the polarization-state distribution of the output light field of right circularly polarization (RCP) and linearly polarization (LP) input in the near field line respectively through the stokes parameters [35], as shown in the Figs. 2(a) and 2(b). The result shows that the output polarization-state distribution of any arbitrary LP input passing through the LCPG will circle the equator twice upon the Poincaré Sphere in one period as shown in Fig. 2(d). It is worth mentioning that the phase-difference of the polarization states of the corresponding points (such as points A and E) on the two loops is π rad. Coincidentally, the polarization states of the output beams present a linear spiral pattern with a period half that of LCPGs. For RCP input, all the output polarization-states are concentrated at the South Pole, with the difference being the initial phase. From the experience gained from RCP

input, we can also draw a conclusion that all the output polarization-states are concentrated at the North Pole when LCP illuminates LCPGs.

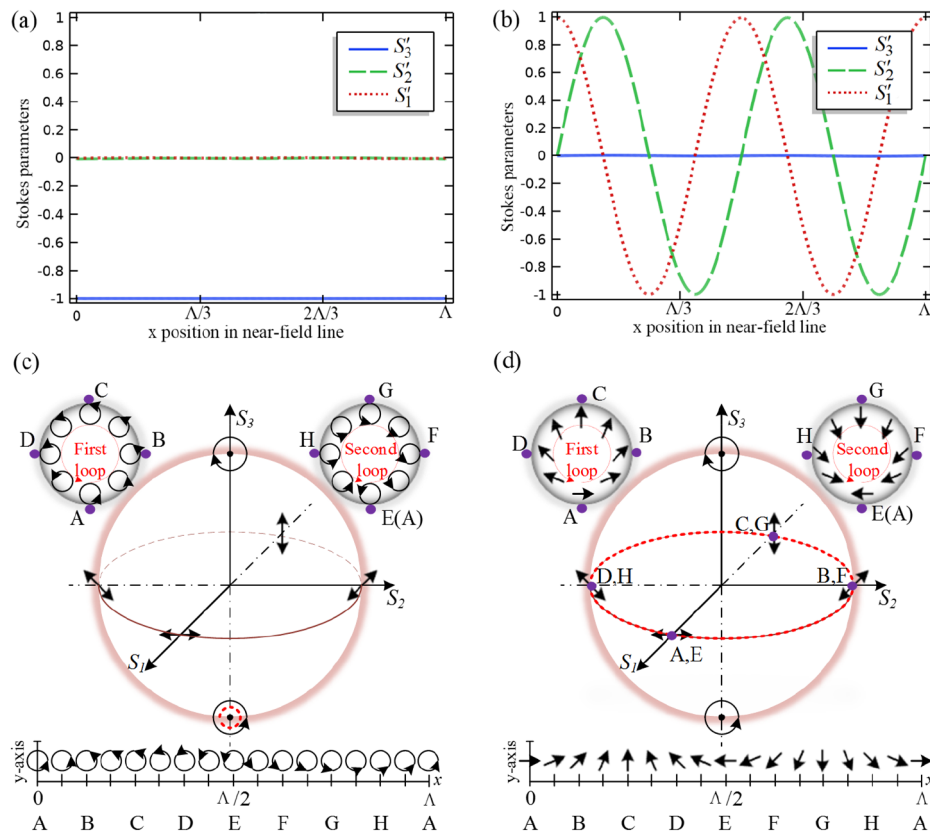


Fig. 2. Stokes parameters in near-field of LCPGs with half-wave retardation with (a) RCP input; (b) LP input. The polarization-state distribution of near-field line on Poincaré Sphere with (c) RCP input; (d) LP input.

2.2. Special cycloidal diffractive quarter waveplate and LPGs

Prior attention was focused on changing the polarization state of uniformly polarized light, while hardly concentrated on modulating the one of non-uniformly polarized light. We all know that a waveplate enables change the polarization state of an illuminated light wave, so it is realizable to design a special waveplate for vector beams to change their polarization state. As mentioned above, the output of LCPGs in near-field possesses a pitch with half of that of LCPGs. So, we can search for a special optical element to modulate the polarization-state from LCPGs. In this paper, we initially demonstrate a special cycloidal diffractive quarter waveplate (CQWP) to modulate the polarization state of near-field output from LCPGs. The CQWP borrows from LCPGs in structure, but its thickness d' requires only quarter-wave retardation and its period Λ' is customized to half the grating period ($\Lambda' = \Lambda/2$) to match the polarization distribution of the near-field.

A schematic of the proposed LPG shows in Fig. 3. The incident beams illuminate along the z-direction.

Jones matrix [36] plays a significant role in the research of polarization optical elements because of its simplicity and power. For paraxial approximation, the Jones matrix of LCPGs

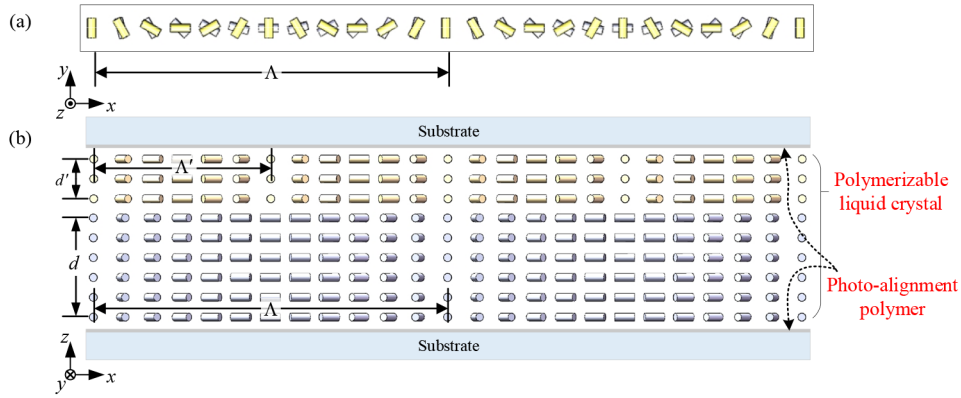


Fig. 3. A schematic diagram of the proposed LPG. (a) Top-view. (b) Side-view. First layer represents the LCPG with a thickness of half-wave retardation, and second layer signifies the CQWP with a thickness of quarter-wave retardation and a period half of the LCPG.

with half-wave retardation can be rewritten by

$$T_1 = \frac{1}{2} \left(\exp(i2\varphi) \begin{bmatrix} -i & -1 \\ -1 & i \end{bmatrix} + \exp(-i2\varphi) \begin{bmatrix} -i & 1 \\ 1 & i \end{bmatrix} \right) \quad (5)$$

We can express the Jones matrix of the CQWP as follows

$$T_2 = \frac{\sqrt{2}}{2} \begin{bmatrix} 1 & 0 \\ 0 & 1 \end{bmatrix} + \frac{\sqrt{2}}{4} \left(\exp(i2\varphi') \begin{bmatrix} -i & -1 \\ -1 & i \end{bmatrix} + \exp(-i2\varphi') \begin{bmatrix} -i & 1 \\ 1 & i \end{bmatrix} \right) \quad (6)$$

where $\varphi' = \pi x / \Lambda' = 2\pi x / \Lambda$ (More precisely, $\varphi' = \varphi_0 + \pi x / \Lambda'$, where φ_0 is the initial azimuth between the LCPG and the CQWP at position $x=0$. We can make φ_0 equal to zero by picking the appropriate origin of coordinates). Eventually, the total transfer matrix is simplified as follows

$$T_{total} = T_2 \cdot T_1 = \frac{1}{2} \left(\exp(i2\varphi) \begin{bmatrix} -1 & -1 \\ i & i \end{bmatrix} + \exp(-i2\varphi) \begin{bmatrix} -1 & 1 \\ -i & i \end{bmatrix} \right) \quad (7)$$

where a constant phase is omitted.

We assume an infinite grating and calculate the far-field electric field E_{out} for each diffraction order by means of the Fourier transform of the near-field output. Then we can express the far-field electric field of the diffraction order as follows

$$E_{out} = \frac{1}{\Lambda} \int_0^\Lambda T_{total} E_{in} e^{-i2\pi mx / \Lambda} dx. \quad (8)$$

We can solve the diffraction efficiency defined by the ratio of output to input intensity $\eta_m = (|E_{out,m}| / |E_{in}|)^2$ as

$$\eta_{\pm 1} = \frac{1}{2} (1 \pm S'_2). \quad (9)$$

where $S'_2 = S_2 / S_0$ is normalized stokes parameter. Furthermore, the conclusion can be drawn that the diffraction efficiency associates with the orientation angle of polarization state.

Considering an LP input $\begin{pmatrix} E_x \\ E_y \end{pmatrix} = \begin{pmatrix} \cos \alpha \\ \sin \alpha \end{pmatrix}$ (where α is the azimuth angle from x-axis), when it propagates through the LPG, only +1st and -1st orders occur and exhibit orthogonal circularly polarized states. Figure 4 shows that the y component of the instantaneous E near-field in FEM simulation for the LPG with $\varphi_0=0$. We find that 45° and 135° LP input deflect to a single order for LPGs with $\varphi_0=0$ (It means that the polarization direction of incidence lights producing a single order is related to φ_0), and all of polarization state must be separated to 45° and 135° LP, including RCP and LCP input lights. Figure 5 shows diffraction properties of the LPG with $\varphi_0=0$ as a function of the azimuth angle of linearly polarization input. Whenever the LP lights with $\alpha = 45^\circ$ or 135° propagates to the LPG, the diffraction efficiency of the ± 1 st order is $\sim 100\%$. Other input lights need to be decomposed into two linear components (45° and 135°) and split to ± 1 st order, respectively.

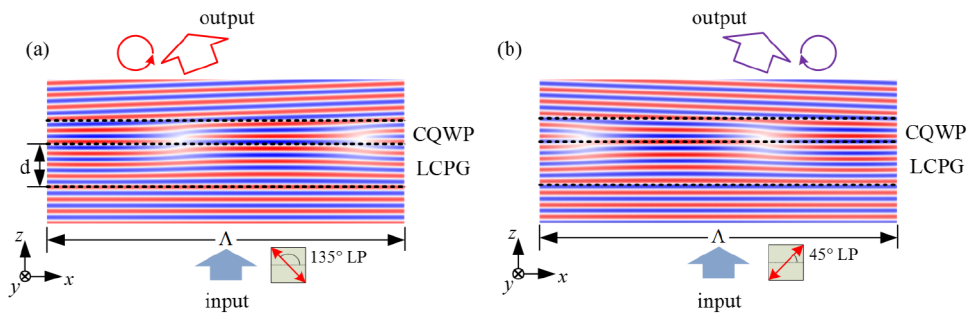


Fig. 4. The y component of the instantaneous E near-field in FEM simulation for the LPG with $\varphi_0=0$: (a) 135° LP input and (b) 45° LP input.

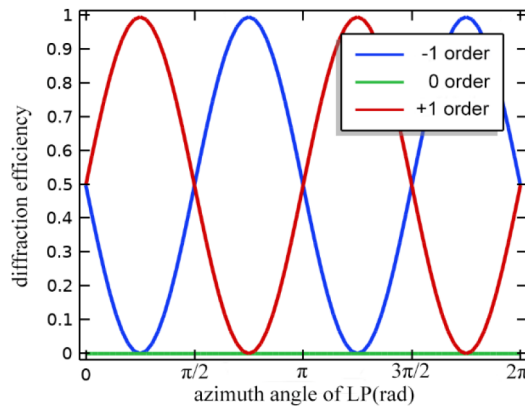


Fig. 5. Diffraction properties of the LPG with $\varphi_0=0$ as a function of the azimuth angle of linearly polarization input (Unit: rad).

By monitoring the polarization-state evolution in near-field, we demonstrate the optional principle of polarization-state modulation and then explain the deflection angle and the output polarization-state of LPGs. For 135° LP input, when passing through an LPG with $\varphi_0=0$, difference-phase LCP output will be obtained as shown in Fig. 6(a). Subsequently, the tilted equiphase surface is formed like blazed gratings. And the deflector angle can be calculated by equation $\tan \theta = \lambda/\Lambda$, which can be explained in Fig. 6(a). And we think the equation is much more accurate than Eq. (4). For RCP or LCP input, the output in near-field is different-azimuth LP

varying continually with spatial pitch Λ , or period $\Lambda/2$ (equal to half of LCPGs). These different-azimuth LP outputs can be decomposed into two beams with equal intensity of orthogonal circular polarization and each of them will generate the tilted equiphase surface (Fig. 6(b)). If the thickness $d/2$ dissatisfies the quarter-wave retardation, there will exist zero-order transmission.

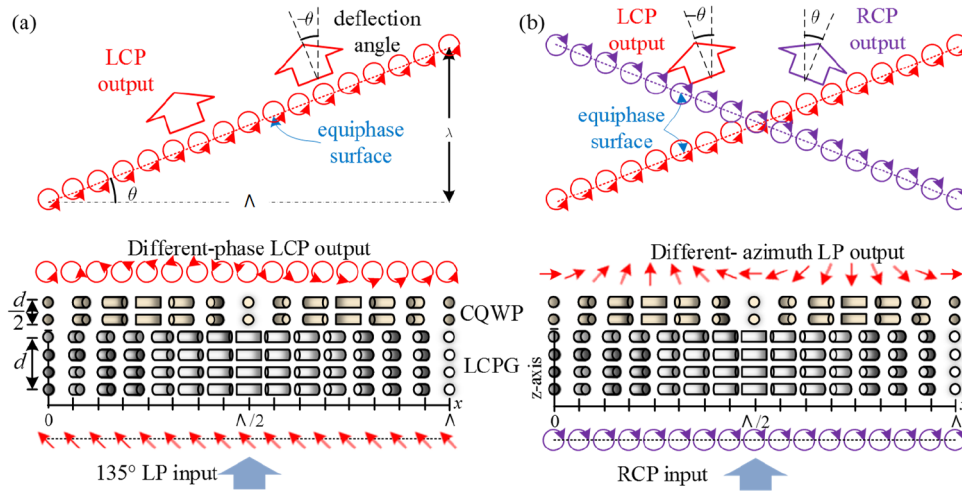


Fig. 6. Illustrates the optional principle of polarization-state modulation and deflection angle of LPGs with $\varphi_0=0$. (a) 135° LP input; (b) RCP input.

3. Experimental procedure

The LPG consists of an LCPG and a CQWP, both of which can be fabricated by polarization holography alignments. Firstly, a thin linearly photo-alignment polymer (LPP) is spin-coated on a transparent substrate at 2000 rpm for 40 seconds, and then the LPP films are dried in an oven at 120°C for several minutes. Secondly, the LPP is exposed to the polarization holographic light-field formed by the superposition of two coherent orthogonal circular polarization beams. The crossing angle of two polarization beams needs to be calculated from formula $\sin \Theta = \lambda_{\text{exp}} / (2\Lambda)$, where λ_{exp} is the wavelength used to expose. After a few minutes of exposure, a spatially varying linear polarization distribution is generated on the substrate. Thirdly, an LC polymer film is spin-coated on the LPP layer, and the LC polymer molecules self-align to the LPP molecules. In order to accurately control the thickness of the LC polymer layer to achieve half-wave and quarter-wave retardation, we require coating multiple thin LC polymer layers.

In this work, the grating periods of the LCPG and the CQWP are set to $30\ \mu\text{m}$ and $15\ \mu\text{m}$, respectively. We use ROP (108-302) as LPP and ROF (5196-417) with a concentration of 80% by weight as LC polymer. The solution is spin-coated on the LPP layer at 3000 rpm for 30 s. Repeat this process until the thickness requirement is met. For convenience, we spin four layers ROF solution to achieve the half-wave retardation (532 nm) and two layers to realize the quarter-wave retardation (532 nm).

The difficulty that how to detect the quarter-wave retardation can be solved through measuring diffraction efficiency of 0th and ± 1 st orders. Specifically, when an LP input passes through the LCPG with quarter-wave retardation, the zero-order is twice the diffraction efficiency of positive or negative first-order, while for an RCP or LCP input, only zero-order and one of the first-orders appear, accounting for 50% of diffraction efficiency respectively. The schematic experimental setup for measuring diffraction efficiency is shown in Fig. 7. The 532 nm laser can be converted

to circularly polarization beams via quarter-wave plate, then diffracted by PGs and detected by power-meter.

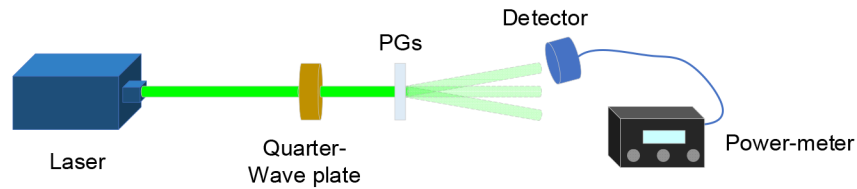


Fig. 7. The schematic experimental setup for measuring the diffraction efficiency.

Figure 8 shows the micrographs of the LCPGs, where one bright-dark fringe means one period. It can be seen from the micrographs that the gratings have good topography and few defects. And Fig. 9 shows the measurements of LCPGs with half-wave and quarter-wave retardation. The sum of +1st and -1st orders diffraction of the two LCPGs can be achieved 99.86% and 49.93% respectively. Both LCPGs satisfy the requirement in terms of thickness. This means that it is feasible to control the thickness by rotating speed and the concentration of LC.

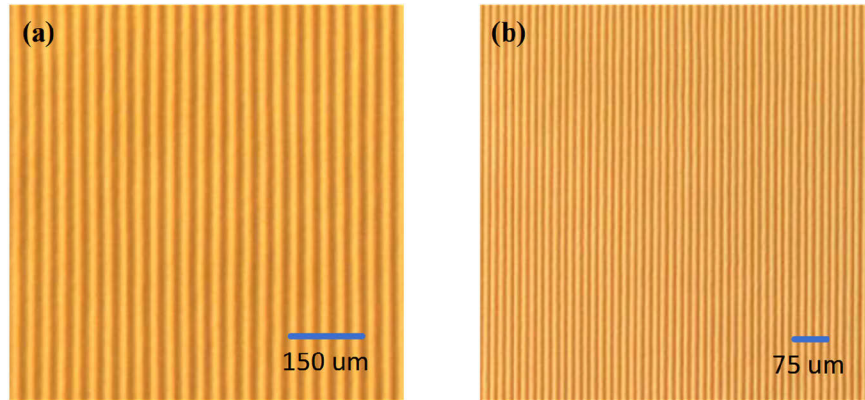


Fig. 8. The micrographs of the LCPGs (one bright-dark fringe means one period). (a) half-wave and period $\Lambda=30 \mu\text{m}$; (b) quarter-wave and period $\Lambda=15 \mu\text{m}$.

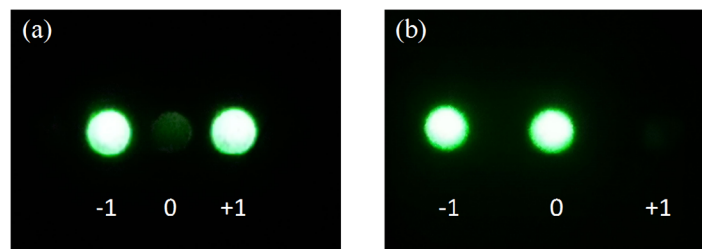


Fig. 9. The diffraction patterns of LCPGs with: (a) half-wave retardation and LP input; (b) quarter-wave retardation and RCP input.

4. Results and discussion

For convenience, a red script L is marked in the lower left corner of the LCPG and the CQWP as shown in Fig. 10. To confirm the properties of LPGs, we should clip the LCPG and the CQWP

together to ensure that the sides of the LC polymer layers are tightly attached. Specifically, stack them as shown in Fig. 10(b).

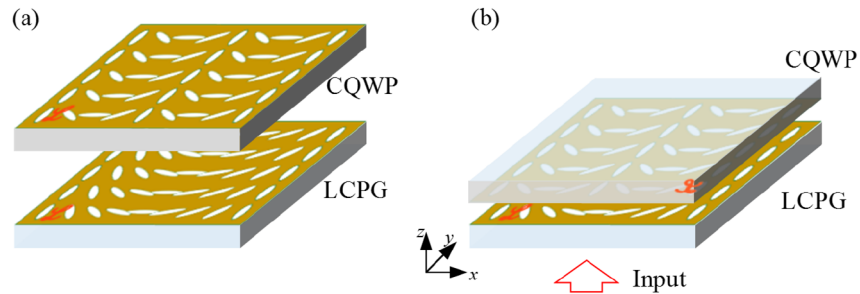


Fig. 10. The schematic diagram about LPGs. (a) the LCPG and the CQWP (the red script L is used to determine the relative position and direction) and (b) correct placement between the LCPG and the CQWP.

Figure 11 illustrates two possible deviations when an LCPG and a CQWP combine to form an LPG. The improper azimuth β will cause the properties of LPGs to disappear, while the initial azimuth φ_0 of LC molecules at $x=0$ resulting from the transverse displacement will only determine the directions decomposed into two linear components. Different azimuth β between the LCPG and the CQWP will generate different diffraction pattern. If the azimuth satisfies $\beta=180^\circ$, the diffraction pattern will be what is shown in Fig. 12. Only when the azimuth between the two gratings is exactly 0° can the properties of LPGs appear. However, the initial azimuth φ_0 of LC molecules at $x=0$ caused by the lateral displacement of the two gratings does not essentially change the characteristics of LPGs. We simulate the response curves of the efficiency of 45° LP input with the initial azimuth φ_0 at $x=0$. The result shows that the initial azimuth φ_0 is related to the LP input direction which retains only one order (Fig. 13). For example, the LPG with initial azimuth $\varphi_0=0^\circ$ can split the orthogonal linear polarizations (45° and 135°) as ± 1 st order diffraction lights. And the LPG with the initial azimuth $\varphi_0=45^\circ$ can split the orthogonal linear polarizations (0° and 90°) as ± 1 st order diffraction lights. When LPGs with the initial azimuth $\varphi_0=45^\circ$ is illuminated by 45° LP lights, the diffraction efficiency of both +1st and -1st orders accounts for 50% as shown in Fig. 13.

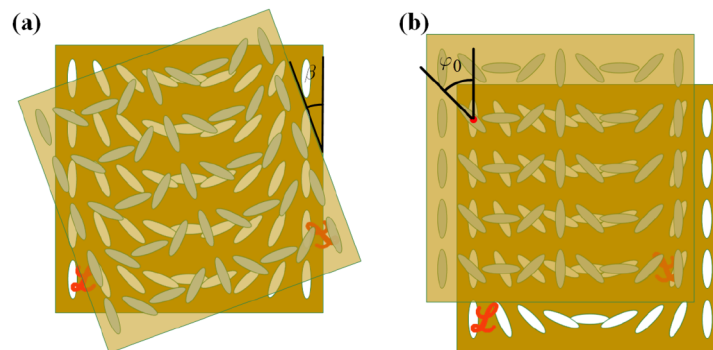


Fig. 11. The illustrations of (a) the azimuth β between the LCPG and the CQWP (b) the initial azimuth φ_0 of liquid crystal molecules caused by the lateral displacement of the two gratings.

To our disappointment, when we combine the thickness-consistent LCPG and CQWP (Figs. 8 and 9) to form LPGs, the interference fringes appear and could not be removed (Fig. 14). We

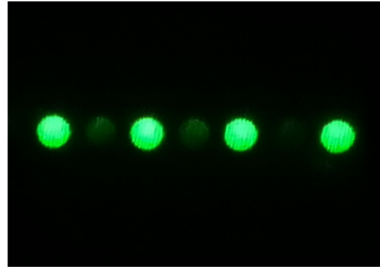


Fig. 12. The diffraction pattern when the azimuth β between the LCPG and the CQWP is $\beta=180^\circ$.

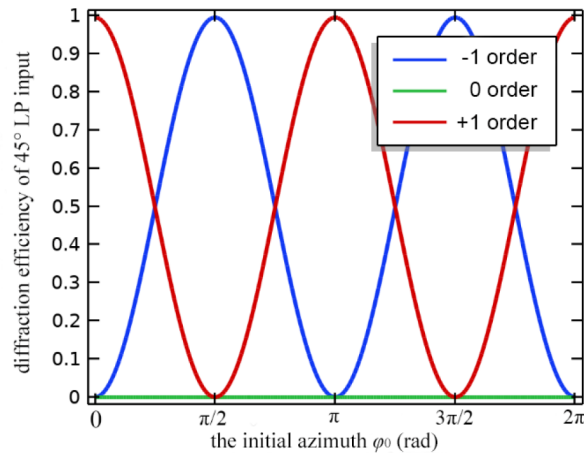


Fig. 13. Diffraction efficiency as a function of the initial azimuth φ_0 when the 45° LP input illuminates the LPG.

guess that the periods of the LCPG and the CQWP are not strictly satisfied due to the insufficient precision of our polarization holographic device, However, the period mismatch cannot be measured accurately in micrographs.

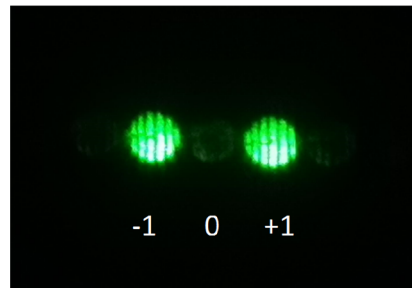


Fig. 14. Interference fringes observed when the periods of the LCPG and the CQWP are unmatched.

In many experiments, we found few combinations with LCPGs and CQWPs that could eliminate interference fringes. What is depressing about the energy ratio of the better CQWP is measured at 58.0%, where the energy ratio is defined by $\zeta = I_0 / (I_{+1} + I_{-1} + I_0)$. The result shows that the maximum efficiency of the LPG is 86%, where the efficiency is defined by the equation

$\eta_m = I_m / (I_{+1} + I_{-1})$, $m = \pm 1$. The main reason for the low efficiency is that the thickness of the CQWP (The thickness is a little thin.) does not meet the quarter-wave retardation. Further by spinning ROP solution, the energy ratio of the CQWP reach 49.81% and the efficiency of the LPG can reach 96.7% as shown in Fig. 15. The possible reasons why one of +1st and -1st orders cannot be eliminated completely include the two periods mismatch and the defect in gratings, etc. The experimental results above confirm the correctness of the LPG theory and simulation.

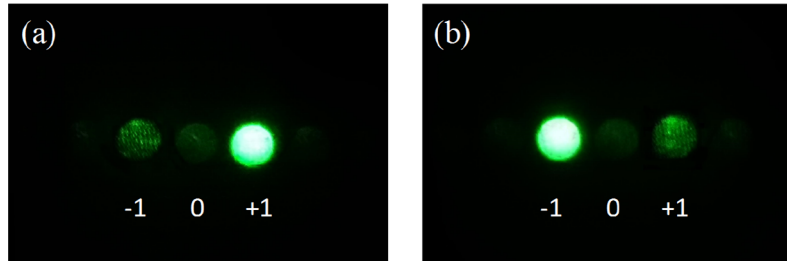


Fig. 15. The diffraction patterns of LPGs with (a) 45° LP input and (b) 135° LP input.

In brief, period matching and thickness control are two challenges in fabricating LPGs.

5. Conclusion

In this paper, we demonstrate a linear polarization grating (LPG) consisting of an LCPG and a CQWP. LPGs can change the ratio of positive and negative first-order diffraction lights by changing the direction of polarization of LP input, while LCPGs need change input polarization with different ellipticity angle. It is convenient for LPGs to split an incident linear polarized beam into two proportionally controllable left- or right-handed circularly polarized light at a certain angle, because we have no need to convert linear polarization to circular polarization with a quarter waveplate like LCPGs. We build a rigorous simulation model to confirm the properties of LPGs. Then we use polarization holography alignments to fabricate an LPG. The experimental results show the sensitivity of the LPG to the polarization direction of an LP input, and the maximum extinction ratio can reach 96.7%. The main reasons why the experimental results are lower than the theoretical value include the deviation of two periods, the defect in gratings and the thickness unmatching. There are two major challenges in making LPGs: period matching and thickness control. Because of polarization-sensitive and deflectable for beams, the LPG could be expected to be applied in polarization beam splitters, optical telecommunications, polarization switch, non-mechanical beam steering and so on.

Funding

National Natural Science Foundation of China (11604327, 11974345, 61475152, 61975202).

Acknowledgments

The authors are indebted to Rolic Company for their kind support with the photo-alignment material. This work was supported by the National Natural Science Foundation of China and State Key Laboratory of Applied Optics, Changchun Institute of Optics, Fine Mechanics and Physics, Chinese Academy of Sciences.

Disclosures

The authors declare no conflicts of interest.

References

1. M. Martinelli and P. Vavassori, "A geometric (Pancharatnam) phase approach to the polarization and phase control in the coherent optics circuits," *Opt. Commun.* **80**(2), 166–176 (1990).
2. H. W. Chen, J. H. Lee, B. Y. Lin, S. Chen, and S. T. Wu, "Liquid crystal display and organic light-emitting diode display: present status and future perspectives," *Light: Sci. Appl.* **7**(3), 17168 (2018).
3. M. V. Berry, "The adiabatic phase and Pancharatnam's phase for polarized light," *J. Mod. Opt.* **34**(11), 1401–1407 (1987).
4. G. P. Crawford, J. N. Eakin, M. D. Radcliffe, A. Callan-Jones, and R. A. Pelcovits, "Liquid-crystal diffraction gratings using polarization holography alignment techniques," *J. Appl. Phys.* **98**(12), 123102 (2005).
5. T. Todorov, L. Nikolova, and N. Tomova, "Polarization holography. 1: A new high-efficiency organic material with reversible photoinduced birefringence," *Appl. Opt.* **23**(23), 4309–4312 (1984).
6. T. Todorov, L. Nikolova, and N. Tomova, "Polarization holography. 2: Polarization holographic gratings in photoanisotropic materials with and without intrinsic birefringence," *Appl. Opt.* **23**(24), 4588–4591 (1984).
7. I. Vartiainen, J. Tervo, J. Turunen, and M. Kuittinen, "Surface-relief polarization gratings for visible light," *Opt. Express* **18**(22), 22850–22858 (2010).
8. M. N. Miskiewicz and M. J. Escuti, "Direct-writing of complex liquid crystal patterns," *Opt. Express* **22**(10), 12691–12706 (2014).
9. K. Hisano, M. Aizawa, M. Ishizu, Y. Kurata, W. Nakano, N. Akamatsu, C. J. Barrett, and A. Shishido, "Scanning wave photopolymerization enables dye-free alignment patterning of liquid crystal," *Sci. Adv.* **3**(11), e1701610 (2017).
10. K. Hisano, M. Ota, M. Aizawa, N. Akamatsu, C. J. Barrett, and A. Shishido, "Single-step creation of polarization gratings by scanning wave photopolymerization with unpolarized light," *J. Opt. Soc. Am. B* **36**(5), D112–D118 (2019).
11. W. Hao, H. Wei, H. Hu, X. Lin, Z. Ge, J. W. Choi, V. Chigrinov, and Y. Lu, "Arbitrary photo-patterning in liquid crystal alignments using DMD based lithography system," *Opt. Express* **20**(15), 16684–16689 (2012).
12. N. V. Tabiryan, S. V. Serak, S. R. Nersisyan, D. E. Roberts, B. Y. Zeldovich, D. M. Steeves, and B. R. Kimball, "Broadband waveplate lenses," *Opt. Express* **24**(7), 7091–7102 (2016).
13. K. J. Hornburg, X. Xiang, J. Kim, M. W. Kudenov, and M. J. Escuti, "Design and fabrication of an aspheric geometric-phase lens doublet," *Proc. SPIE* **10735**, 1073513 (2018).
14. C. Provenzano, P. Pagliusi, and G. Cipparrone, "Highly efficient liquid crystal based diffraction grating induced by polarization holograms at the aligning surfaces," *Appl. Phys. Lett.* **89**(12), 121105 (2006).
15. H. Sarkissian, S. V. Serak, N. V. Tabiryan, L. B. Glebov, V. Rotar, and B. Y. Zeldovich, "Polarization-controlled switching between diffraction orders in transverse-periodically aligned nematic liquid crystals," *Opt. Lett.* **31**(15), 2248–2250 (2006).
16. C. Oh and M. J. Escuti, "Achromatic diffraction from polarization gratings with high efficiency," *Opt. Lett.* **33**(20), 2287–2289 (2008).
17. Y. Weng, D. Xu, Y. Zhang, X. Li, and S. T. Wu, "Polarization volume grating with high efficiency and large diffraction angle," *Opt. Express* **24**(16), 17746–17759 (2016).
18. K. Gao, C. McGinty, H. Payson, S. Berry, J. Vornehm, V. Finnmeyer, B. Roberts, and P. Bos, "High-efficiency large-angle Pancharatnam phase deflector based on dual-twist design," *Opt. Express* **25**(6), 6283–6293 (2017).
19. B. Y. Wei, S. Liu, P. Chen, S. X. Qi, and J. L. Zhao, "Vortex Airy beams directly generated via liquid crystal q-Airy-plates," *Appl. Phys. Lett.* **112**(12), 121101 (2018).
20. M. J. Escuti and W. M. Jones, "39.4: Polarization-independent switching with high contrast from a liquid crystal polarization grating," *Dig. Tech. Pap. - Soc. Inf. Disp. Int. Symp.* **37**(1), 1443–1446 (2006).
21. G. Cincotti, "Polarization gratings: design and applications," *IEEE J. Quantum Electron.* **39**(12), 1645–1652 (2003).
22. J. Kim, C. Oh, M. J. Escuti, L. Hosting, and S. Serati, "Wide-angle nonmechanical beam steering using thin liquid crystal polarization gratings," *Proc. SPIE* **7093**, 709302 (2008).
23. J. Kim, R. K. Komanduri, K. F. Lawler, D. J. Kekas, and M. J. Escuti, "Efficient and monolithic polarization conversion system based on a polarization grating," *Appl. Opt.* **51**(20), 4852–4857 (2012).
24. E. Nicolescu and M. J. Escuti, "Polarization-independent tunable optical filters based on liquid crystal polarization gratings," *Proc. SPIE* **6654**, 665405 (2007).
25. H. Chen, Y. Weng, D. Xu, N. V. Tabiryan, and S. T. Wu, "Beam steering for virtual/augmented reality displays with a cycloidal diffractive waveplate," *Opt. Express* **24**(7), 7287–7298 (2016).
26. Y. H. Lee, G. Tan, T. Zhan, Y. Weng, G. Liu, F. Gou, F. Peng, N. V. Tabiryan, S. Gauza, and S. T. Wu, "Recent progress in Pancharatnam–Berry phase optical elements and the applications for virtual/augmented realities," *Opt. Data Process. Storage* **3**(1), 79–88 (2017).
27. R. K. Komanduri, W. M. Jones, C. Oh, and M. J. Escuti, "Polarization-independent modulation for projection displays using small-period LC polarization gratings," *J. Soc. Inf. Disp.* **15**(8), 589–594 (2007).
28. V. Presnyakov, K. Asatryan, T. Galstian, and V. Chigrinov, "Optical polarization grating induced liquid crystal micro-structure using azo-dye command layer," *Opt. Express* **14**(22), 10558–10564 (2006).
29. M. Ishiguro, D. Sato, A. Shishido, and T. Ikeda, "Bragg-Type Polarization Gratings Formed in Thick Polymer Films Containing Azobenzene and Tolane Moieties," *Langmuir* **23**(1), 332–338 (2007).
30. A. Shishido, "Rewritable Holograms Based on Azobenzene-containing Liquid-crystalline Polymers," *Polym. J.* **42**(7), 525–533 (2010).

31. J. Tervo and J. Turunen, "Paraxial-domain diffractive elements with 100% efficiency based on polarization gratings," *Opt. Lett.* **25**(11), 785–786 (2000).
32. J. A. Davis, J. Adachi, C. R. Fernández-Pousa, and I. Moreno, "Polarization beam splitters using polarization diffraction gratings," *Opt. Lett.* **26**(9), 587–589 (2001).
33. E. Hasman, Z. E. Bomzon, A. Niv, G. Biener, and V. Kleiner, "Polarization beam-splitters and optical switches based on space-variant computer-generated subwavelength quasi-periodic structures," *Opt. Commun.* **209**(1-3), 45–54 (2002).
34. J. Kim, Y. Li, M. N. Miskiewicz, C. Oh, M. W. Kudenov, and M. J. Escuti, "Fabrication of ideal geometric-phase holograms with arbitrary wavefronts," *Optica* **2**(11), 958–964 (2015).
35. B. Schaefer, E. Collett, R. Smyth, D. Barrett, and B. Fraher, "Measuring the Stokes polarization parameters," *Am. J. Phys.* **75**(2), 163–168 (2007).
36. R. C. Jones, "A new calculus for the treatment of optical systems I. description and discussion of the calculus," *J. Opt. Soc. Am.* **31**(7), 488–493 (1941).